Unidirectional shear horizontal wave generation by periodic permanent magnets electromagnetic acoustic transducer with dual linear-coil array

Alan C. Kubrusly, Lei Kang, Iury S. Martins and Steve Dixon

***Abstract*— Shear horizontal (SH) waves are commonly generated by periodic permanent magnet (PPM) electromagnetic acoustic transducers (EMATs) in metallic media. Conventional PPM EMATs generate ultrasonic waves, which simultaneously propagate both forwards and backwards. This can be an undesirable characteristic, since the backward wave can be eventually reflected, reaching the receiver transducer where it can mix with the signal of interest. This limitation can be overcome using two side-shifted PPM arrays and racetracks coils to generate SH waves in a single direction. That design relies on the EMAT's wavefront diffraction to produce constructive and destructive interference, but produces unwanted backward travelling side-lobes. Here we present a different design, which uses a conventional PPM array and a dual linear-coil array. The concept was numerically simulated, the main design parameters were assessed and the unidirectional EMAT was experimentally evaluated on an aluminum plate, generating the SH0 guided wave mode nominally in a single direction. The amplitude ratio of the generated waves at the enhanced to the weakened side is above 20 dB. Since the wavefronts from the two sources are perfectly aligned, no obvious backward side-lobes are present in the acoustic field, which can significantly reduce the probability of false alarm of an EMAT detection system.**

***Index Terms*— Electromagnetic acoustic transducers; unidirectional generation; shear horizontal waves; guided waves**

I. Introduction

SHEAR horizontal (SH) waves are widely used for defect inspection in plates and pipes [1, 2, 3, 4, 5, 6, 7] due to its advantages, such as simple dispersion relationship, the possibility of readily operating with a single non-dispersive mode and no energy loss due to non-viscous liquid loading. SH waves can be generated either by a periodic permanent magnet (PPM) electromagnet acoustic transducers (EMATs), shear-polarized piezoelectric strips [8, 9, 10] or by magnetostrictive patch transducers [11]. The former has the remarkable advantage of not requiring contact with the sample, whereas the others have to be properly bonded to the surface of the sample [7].

Conventional PPM EMATs generate SH waves that propagate both forwards and backwards. This can complicate the interpretation of the received signal, since the backward propagated wave can be eventually reflected or directly arrive at the receiver due to a closed-loop propagation path, like circumferential inspection of pipes [1], being thus mixed with the signal of interest. Therefore, unidirectional generation provides a more reliable inspection.

Efficient unidirectional generation of ultrasonic waves is possible if two ultrasonic sources are separated by a predefined distance and excited with the proper delay so, constructive interference occurs in one propagation direction, whilst destructive interference occurs in the opposite direction. This principle has been used for many years [12] for unidirectional generation, for several types of ultrasonic guided wave modes. Yamasaki et al [13] used an EMAT with two spaced coils to generate guided waves in a single direction in a steel wire. Zhu and Rose [14, 15] used an array of piezoelectric elements, either with four or two elements per period, exciting each element with the proper delay to generate unidirectional Lamb waves in an aluminum plate, reaching 90% cancelation of the waves generated to the unwanted side. Then, the same concept was extended to unidirectional generation of axisymmetric longitudinal guided waves in pipes with an array, where each element consists of several piezoelectric elements around the pipe forming a ring [16]. Two or three rings of piezoelectric transducers were used to generate longitudinal [17] and torsional [18, 19, 20] guided waves in pipes in a single direction.

Recently Chen et al. [9] predominantly generated SH waves in a single direction with two pairs of thickness-shear piezoelectric strips. The separation of piezoelectric strips in each pair was half-wavelength, and one pair was separated from the other by a quarter-wavelength; the second pair was excited by a 90^o delayed signal. Two separations between strips were used, either 4 mm or 8 mm; the former was excited at 196 kHz and the latter at 98 kHz, providing generated SH waves in the unwanted direction with 15% and 20% of the amplitude of the wave generated to the desired direction, respectively.

Unidirectional generation is more conveniently achieved if

This work was supported in part the Brazilian National Council for Scientific and Technological Development, CNPq, by the Coordenação de Aperfeiçoamento de Pessoal de Nível Superior - Brasil (CAPES) - Finance Code 001, by the Carlos Chagas Filho Foundation for Research Support of Rio de Janeiro State (FAPERJ)

A. C. Kubrusly and I. S. Martins are with Centre for Telecommunication Studies, Pontifical Catholic University of Rio de Janeiro, Rio de Janeiro, 22451-900, Brazil (e-mail: alan@cpti.cetuc.puc-rio.br).

L. Kang is with the School of Energy and Electronic Engineering, University of Portsmouth, Portsmouth, PO1 3DJ, UK (e-mail: lei.kang@port.ac.uk).

S. Dixon is with the Department of Physics, University of Warwick, Coventry, CV4 7AL, UK (e-mail: S.M.Dixon@warwick.ac.uk).

the two ultrasonic sources are produced by the same transducer assembly, since more precise separation of both sources is ensured by the transducer construction. This is readily achieved in some types of EMAT, for instance, with meander-line EMATs where a second coil can be introduced underneath the magnet, as previously used for generating unidirectional Rayleigh and SV waves [21, 22]. This principle however cannot be straightforwardly applied to PPM EMATs to generate unidirectional SH waves, due to the nature of the transducer coil and magnet arrangement. We have recently presented a solution [23] that uses two side-shifted, interlaced racetrack coils and PPM arrays, which produce small but non-negligible side-lobes in the backward propagation direction. Here we propose a new design, which effectively generates SH waves in a single direction and, unlike the previous design, does not present backward propagating side-lobes.

II. Principle of Unidirectional Wave Generation

The principle of unidirectional generation used in this paper is described next, where it is assumed that two generic ultrasonic sources separated by a predefined distance Δx can be excited independently. Consider initially that a monochromatic signal at the frequency f, or angular frequency $\omega = 2\pi f$, is excited from both sources, namely A and B, where the second one is delayed by Δt. Then, the propagated wavefield from each source along the x-axis is, respectively, given by:

$$u_A = e^{j[\omega t \mp \kappa x]}, \tag{1}$$

$$u_B = e^{j[\omega(t+\Delta t) \mp \kappa(x+\Delta x)]}, \tag{2}$$

where $\kappa = 2\pi/\lambda$ is the wavenumber, with λ being the wavelength, and the symbol $\mp$ stands for the wave propagating to the right (positive direction of x-axis), upper symbol, and to the left, lower symbol. Without loss of generality, it is considered unit amplitude waves. Setting Δt and Δx to properly match, one can create constructive and destructive interferences at the right and left-hand sides. If the sources are separated by a quarter-wavelength, i.e., $\Delta x = \pi/2\kappa$, and the delay is a quarter-period, or 90º, i.e., $\Delta t = \pi/2\omega$, then the total field at the right and left-hand sides are, respectively:

$$u_+ = e^{j[\omega t - \kappa x]} + e^{j\left[\omega\left(t+\frac{\pi}{2\omega}\right) - \kappa\left(x+\frac{\pi}{2\kappa}\right)\right]} = 2e^{j[\omega t - \kappa x]}, \tag{3}$$

$$u_- = e^{j[\omega t + \kappa x]} + e^{j\left[\omega\left(t+\frac{\pi}{2\omega}\right) + \kappa\left(x+\frac{\pi}{2\kappa}\right)\right]} = 0, \tag{4}$$

showing that the backward propagation is suppressed by destructive interference.

For finite-length pulses, this principle still holds, as schematically shown in Fig. 1, where it is considered the generation of a non-dispersive wave. The copper-color and grey rectangles represent the two independent sources, A and B, which are polarized in order to generate the wave-mode of interest. Since B is shifted to the right, the waves generated by it arrive earlier, compared to those generated by A, for positions at the positive x-axis and later at the negative x-direction. The time delay imposed at B, however, compensates for it, making both to arrive in-phase at the right-hand side and out-of-phase at the left-hand side, hence producing enhanced and weakened waves, respectively.

This principle ideally works for any type of wave, provided that one is able to introduce separated sources along the direction of propagation. Destructive and constructive interferences only occur at the frequency for which the separation equals a quarter-wavelength. In other words, one must obey the relationship $f = c/\lambda$, otherwise, the phase delay does not match the separation and ideal wave suppression does not occur. It is also worth highlighting that the separation between sources can be any odd multiple of $\lambda/4$, as long as time delay matches. However, short separation naturally mitigates any pulse changing phenomenon, such as attenuation and dispersion.

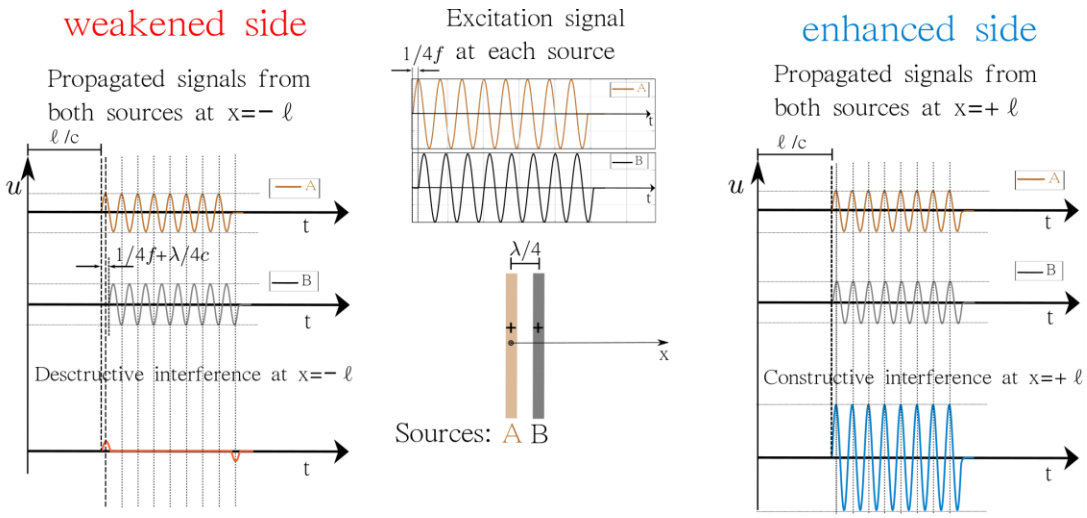

Fig. 1 Principle of operation for unidirectional wave generation with two spaced sources. In the middle, copper-color and grey rectangles represent sources A and B, which generate waves with the polarization of interest. Their respective excitation signals are shown in the top plot with their respective colors. The right-hand side (positive x) is the enhanced side with individual wave's signal and total wave due to the constructive interference. The left-hand side is the weakened side where destructive interference occurs. λ means the wavelength, f the excitation signal frequency, c the wave phase speed and u is the displacement wavefield.

III. Conventional PPM EMAT and SH waves

SH guided waves in plates are polarized in the in-plane z-direction, whilst propagating in the x-direction where the plate surfaces lie in the x-z plane [24]. In this paper, we operate below the first cut-off frequency-thickness, in which only the fundamental SH0 mode propagates. The SH0 mode is non-dispersive, meaning that

$$\kappa = \omega / c_T, \tag{5}$$

or equivalently, the SH0 mode has a constant phase speed equal to the c_T, which is the bulk shear-wave speed in the medium.

In order to generate SH waves, one has to impose shear stress parallel to the plate surface and perpendicular to the propagation direction. SH waves can be efficiently generated with PPM EMATs [7]. A PPM EMAT consists of an array of alternating polarity magnets with a racetrack coil underneath, as shown schematically in Fig.2(a). In a conductive material, the coil induces an eddy current density, $\boldsymbol{J}$, in the skin-depth of the material surface and in the opposite direction to the current injected into the coil, I. Lorentz forces are created in the material given by

$$\boldsymbol{F} = \boldsymbol{J} \times \boldsymbol{B}, \tag{6}$$

where $\boldsymbol{B}$ is the static magnetic from the magnets. The exact nature of the generation mechanism is actually more complicated [25], but the simplified explanation presented above is appropriate for an overview of the Lorentz force generation mechanism here. For a PPM EMAT, according to the adopted Cartesian axes of Fig.2(a), the induced eddy currents in the sample are in the x-direction and the magnet field of each magnet is in the y-direction, with alternate polarities. Thus according to (6), this arrangement generates forces in the z-direction, and consequently SH waves that propagate in the x-direction.

The separation of forces with alternate polarities defines the nominal half-wavelength of the generated waves. However, due to the finite number of spatial periods, a bandwidth of excitable wavenumber exists, instead of a single wavenumber [1, 26]. The specific requirements of the measurement application determine the choice of the number of spatial periodic cycles in the EMAT. Increasing the number of spatial periods narrows the wavenumber bandwidth. Wide bandwidth is useful when generation or reception of several modes is required, such as when analyzing mode conversion phenomenon [4, 5, 27, 28]. However, narrow bandwidth gives improved mode selection capability when several modes are able to propagate [29]. Besides, the strength of the generated wave increases if more spatial periods are added, since more force sources are coherently combined [30], i.e., the waves originated from each element of the array are added in-phase, since they are separated by $\lambda/2$ and have opposite polarities, as shown by Fig.2(a). Nevertheless, the number of periods cannot be indefinitely increased, since the EMAT would be quite large, also giving rise to a high magnetic attraction force when used in ferromagnetic materials, which can be an issue in some applications [3]. Three spatial periods are frequently used, as it produces a fair compromise between the aforementioned restrictions [3, 31, 27, 32, 30, 33].

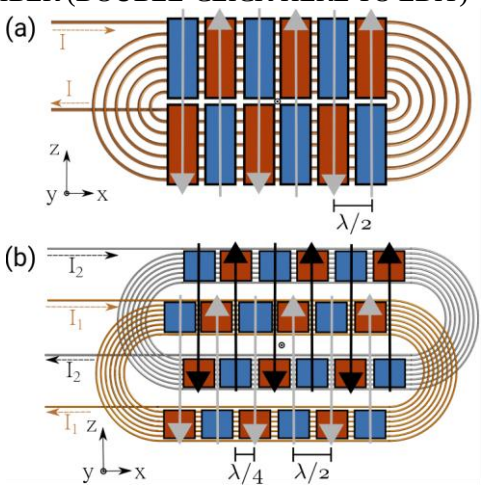

Fig. 2. Conventional PPM EMAT (a) and unidirectional side-shifted PPM EMAT with two racetrack coils presented in [23] (b). Red and blue blocks represent the magnets' poles. The dashed lines represent the current injected into each racetrack coil. Generated Lorentz forces from each array are schematically represented by vertical grey and black arrows.

In order to generate an SH wave mode, the frequency of the excitation current applied to the coils have to match the nominal wavelength according to the dispersion relationship of the mode of interest, given by (5) for the SH0 mode. Similar to how the magnets distribution is related to the wavenumber bandwidth, the temporal profile of the generation current defines a frequency bandwidth. A short-time signal produces a wide-band signal with relatively a small amount of the overall frequency content matching the predefined transducer wavelength. A temporally long drive current of many cycles of a single frequency produces an ultrasonic wave that is poorly time-resolved, and hence hinders identification of scattered waves from the incident one, for instance. The duration of the applied current pulse into the coils also affects the minimum time which the propagated wave can be identified into the received signal, due to the interference of the high-power excitation pulse in the receiving electronics. Usually, a few cycles of a tone-burst current is used as an excitation pulse [3, 6, 21, 32, 34], which provides a compromise between the temporal and frequency specification of the wave generated.

Unidirectional generation, in principle, also holds with transducers that impose an array of sources, such as PPM EMATs, rather than a single source, like illustrated in Fig.1, provided one can excite alternate forces with the proper delay [14]. However, due to the arrangement of the racetrack coil and magnets, shown in Fig.2(a), this is not feasible with conventional PPM EMATs. This constraint was discussed in detail in our previous letter [23], where we presented the solution shown in Fig.2(b) for unidirectional SH generation, with two interlaced PPM arrays and racetrack coils that can accommodate a second array slightly shifted sideways. In the next section, we propose an alternative design of unidirectional SH EMAT, using the conventional PPM array but with a different coil geometry.

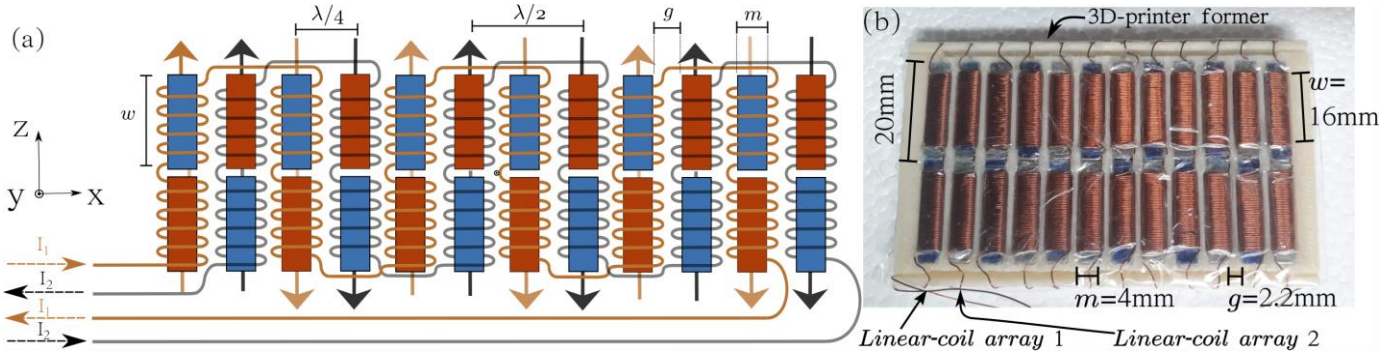

Fig. 3. Design of unidirectional PPM EMAT with dual linear-coil array (a). Red and blue blocks represent the magnets' poles and the linear-coil arrays are represented by copper-color and grey wires. Magnets' length is m and the gap between magnets is g. Each element of the linear-coil arrays is wound around an individual magnet in the correct sense so induced Lorentz forces at the same column have the same direction. Forces generated by the first array are represented by vertical copper-color arrows, whereas the ones related to the second array with black vertical arrows. The dashed lines represent the currents I_1 and I_2 injected into coil arrays 1 and 2, respectively. I_2 is 90º delayed respect to I_1. Photograph of fabricated unidirectional dual linear-coil array SH EMAT with dimensions (b).

IV. DESIGN OF PPM EMAT WITH DUAL LINEAR-COIL ARRAY

In order to introduce two independent ultrasonic sources that are capable of generating SH waves, (i.e., alternate forces along the z-direction and propagation along the x-direction), we use the conventional PPM array layout, but without the usual racetrack coil design. Instead, a dual, linear-coil array is used, as shown in Fig. 3(a). Each element of the linear-coil array consists of a conductive wire wrapped around a single rectangular magnet, which individually operates as a linear-coil EMAT [35, 36, 37]. Note that, similar to Fig.2, the current induced in the skin-depth of the sample still lies in the x-direction, but since there is no racetrack coil underneath the magnets, one is able to associate adjacent magnets with different currents, without the need for shifting half of the magnets sideways. Also, since this EMAT has the classical PPM arrangement of alternating polarities of magnets, it is robust, because attraction forces between adjacent magnets act to form a stable array as a whole. The winding of each element of the coil array has to be alternated between clockwise and counter-clockwise due to the alternate polarity of magnets, as shown in Fig. 3(a). This way, the dual linear-coil array generates the force pattern shown by the vertical arrows. Consecutive forces originated from the same coil array have alternate polarity and thus define a distance of half-wavelength ($\lambda/2$). Consequently, adjacent forces from different coil arrays are separated by a quarter-wavelength ($\lambda/4$). Unidirectional generation is then obtained when exciting the second coil array delayed by 90º as explained in section II.

In this design, as shown in Fig. 3(a), the nominal wavelength is given by

$$\lambda = 4(m + g), \tag{7}$$

where m is the magnet's length and g the gap between magnets. Thus, one can adjust the wavelength by choosing m and g through (7). For a fixed wavelength, keeping the gap short and increasing the magnet's length is preferred since the area where the Lorentz force is generated is larger, and, consequently, the generated waves, stronger. This design, however, requires a non-zero gap between magnets, since the width of the linear coil at the side of each magnet imposes a minimum separation between adjacent magnets. The observations regarding the spatial distribution of the EMAT and characteristics of the excitation signal also hold for the unidirectional generation, since the wave generation phenomenon from each array is the same. It is worth noticing that, in order to introduce the second array a quarter-wavelength separated from the first one, the nominal wavelength of the proposed EMAT is twice that of a conventional PPM EMAT, i.e., $\lambda = 2(m + g)$ as shown in Fig.2(a), for the same magnet's length and gap.

In order to assess the performance of the proposed unidirectional transducer, three-dimensional finite element simulations were performed with a commercial Finite Element solver (PZFlex, currently known as OnScale). The plate was modeled with transverse and longitudinal wave speeds of $c_T = 3075\ m/s$, $c_L = 6374 m/s$, respectively, and material density $\rho = 2698 m/s$. In order to generate the SH0 mode, a set of constant force densities were applied along the z-direction at predefined regions on the surface of the model that correspond to the areas under each magnet and coil element where the Lorentz forces are generated. The assumption of constant force is a good approximation for small lift-off [33, 35, 38], allowing one to generate SH guided waves without including the EMAT coupling mechanism in the numerical simulation, as validated

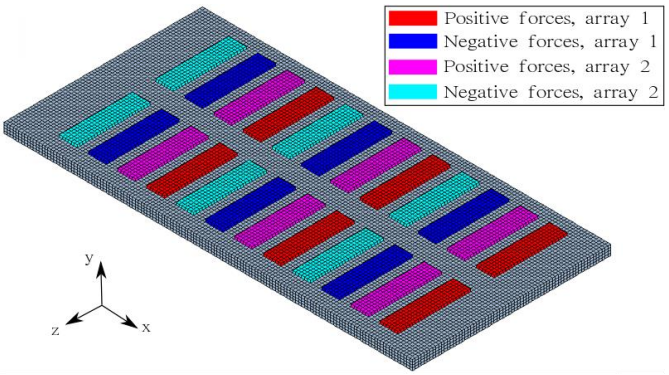

Fig. 4 Detail of 3D-FE mesh and SH wave generation areas. The red and blue rectangles correspond to the regions of positive and negative constant force densities, along the z-direction, for the first array, whereas magenta and cyan rectangles are the positive and negative, respectively, forces for the second array.

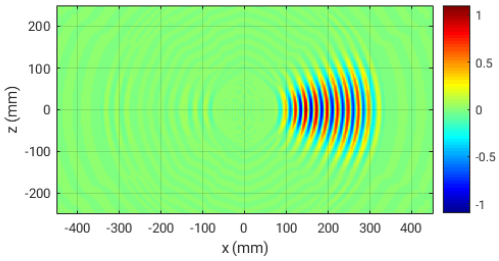

Fig. 5 Snapshot of normalized wavefield at 100 μs at the top surface of the plate.

previously elsewhere [4, 5, 31, 23]. Fig.4 shows the sector of the FE mesh where generation takes place in a 1.5 mm aluminum plate. The colored rectangles are the areas underneath which forces are applied at the interface with the plate, correlating with each magnet and coil pair. The red and blue rectangles correspond, respectively, to positive and negative forces of the first array; whereas magenta and cyan rectangles are the positive and negative forces, respectively, for the second array. Note that the direction of each force along the z-axis follows the vertical arrows in Fig. 3(a), obeying the Lorentz force pattern produced by each linear-coil array. Forces were modulated by an 8-cycle, sinusoidal tone-burst, with a center frequency matching the nominal wavelength through (5), and the ones corresponding to the second array are delayed by a phase shift of 90º, relative to the first, in order to simulate the delayed driving current applied to the second coil array, as schematically shown in the middle of Fig. 1.

Fig. 5 shows a snapshot of the generated wavefield, with three spatial periods when the following dimensions were used: $m = 4$ mm and $g = 2.2$ mm, thus providing a nominal wavelength of approximately $\lambda = 25$ mm, as per (7), and then the frequency was set to 124 kHz. The center of the generation location is at the origin. One can see that it generates an SH wave travelling to the right, with negligibly small amplitude signals travelling to the left.

In order to analyze the effect of the number of spatial periods and the gap between magnets, additional simulations were performed. In each simulation, the amplitude of the generated wave at the enhanced and weakened sides, at a fixed distance of 380 mm from the origin, in the x-axis, were extracted, namely

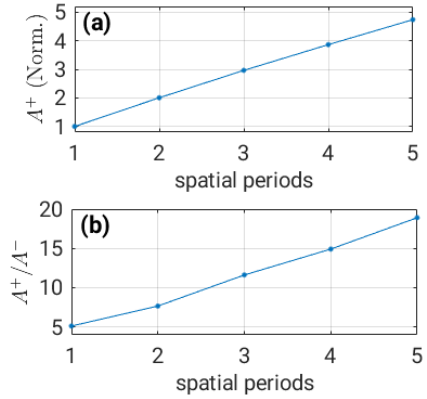

Fig. 6 Normalized amplitude of the enhanced side wave, (a), and the ratio of the amplitude of the generated wave at the enhanced to weakened sides, (b), as a function of the number of magnets' periods.

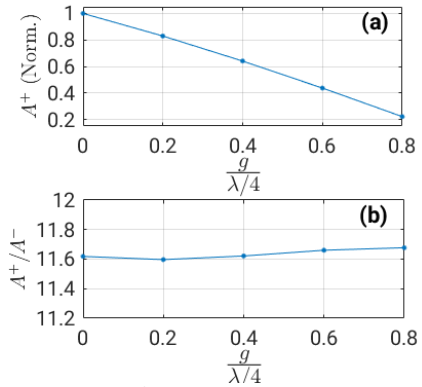

Fig. 7 Normalized amplitude of the enhanced side wave, (a), and the ratio of the amplitude of the generated wave at the enhanced to weakened sides, (b); as a function of the gap per quarter-wavelength between magnets for three periods of magnets. Wavelength is kept constant meaning that increasing gap decreases the magnet length.

A^+ and A^-, respectively. Unidirectionality was calculated by their ratio, that is, A^+/A^-. Fig.6(a) and (b) show the forward amplitude, A^+, and unidirectionality, respectively, when varying the number of spatial cycles, while keeping constant the nominal wavelength, magnets length and gap, with the same dimensions as used in the precedent analysis. In Fig. 6(a) the forward amplitude is normalized per the configuration that presented the lowest amplitude value, namely, just one spatial cycle. As can be seen, increasing the number of cycles increases the amplitude of the forward propagating wave, since more wave-generating elements are coherently added, as expected. Unidirectionality also increases linearly, which means that the amplitude of the suppressed wave on the weakened side does not change, since the wave generated by each array are out-of-phase at the weakened side. Fig. 7 shows similar analysis when the gap was varied while keeping the wavelength constant at 25 mm, by compensating for the length of the magnets as per (7), and using three spatial periods. In Fig.7(a), the forward amplitude was normalized per the configuration that presented the highest value, namely, zero gap. One can observe that, reducing the gap also increases the amplitude of the forward propagating wave since the Lorentz forces are increased, but there is no significant effect on the unidirectionality, since all individual waves are subjected to the same effect.

The simulation analyses presented herein show that the proposed design can unidirectionally generate SH waves effectively. Its efficiency increases with the number of magnets, whereas the role of the magnets' length and the gap between magnets is minor on the wave suppression, provided that all gaps are identical and the time delay of the excitation signal matches the shift between the two arrays.

V. Experimental Validation

The proposed design was fabricated as shown in Fig. 3(b). The length and the width of each magnet are 4 mm and 20 mm, respectively, and the gap between magnets is 2.2 mm, creating a nominal wavelength of approximately $\lambda = 25$ mm, as in the simulations. The coils were hand-wound using an AWG-30 copper wire (diameter of 0.25 mm) with 47 turns around each magnet. Due to winding constraints, the coils start and end 2

mm apart from the ends of each magnet, thus creating an active width for the Lorentz forces of w =16 mm. Three periods of magnets were used, as is often used in conventional PPM EMATs [3, 31, 27, 32], and since it provided enough unidirectionality in the numerical analysis. The magnet and linear-coil array assembly was mounted in a 3D-printer former, to impose better alignment between adjacent magnet-coil pairs, and to fine adjust the gap, so that the wavelength is the same as the nominal wavelength of the commercially available PPM EMAT used for receiving the waves. The main fabrication steps can be summarized as follows. Firstly, the wire was wound around the first magnet and a thin auto-adhesive tape was wrapped around the magnet and coil so the coils remain fixed around the magnet. Then, the wire is wound around another magnet, in the opposite sense, and is also fixed with auto-adhesive tape. These two magnets and coils form the first column in Fig. 3, and are then inserted into the first row of the 3D-printer former. These steps are repeated for all the odd-order columns of Fig. 3, which correspond to the first array. Finally, all the steps are performed for the even-order columns to complete the transducer.

To experimentally assess the proposed design, a two-channel signal generator synthesized two 8-cycles tone-bursts at 124 kHz, being the second one 90º phase-shifted, similar to numerical simulation. The duration of the exciting pulse also provides a fairly short signal and allows that the propagated wave could be clearly separated from the excitation pulse at the receiver distance. The signals were power amplified and then connected to each linear-coil array of the unidirectional transducer, which was placed in the middle of a 1.5 mm thick aluminum plate. The EMAT was placed in contact with the sample in order to minimize the lift-off. A conventional 3 cycle, 25 mm nominal wavelength PPM EMAT from Sonemat Ltd. was used as a receiver, which was connected to the amplifier prior to displaying its signal on an oscilloscope and recording its waveform. The receiver was placed at several angular positions, at a fixed distance from the transmitter of 380 mm, so the directivity of the EMAT could be assessed. No significant temperature increase on the coils was observed during operation.

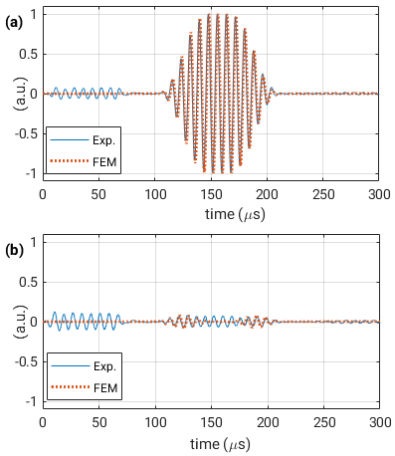

Fig. 8 Numerical, dotted line, and experimental, continuous line, received signals at x=+380 mm (a) and x= -380 mm (b). Amplitude is normalized per the maximum value of the received signal at the enhanced side. The signal for times around 50μs is the electrical interference from the driving current, and is therefore present only in experimentally measurements.

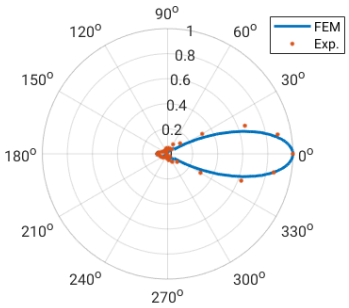

Fig. 9 Numerical, solid line, and experimental, red dots, directivity diagram for the unidirectional PPM EMAT with dual linear-coil array. Either in experiments or simulation, the received signal used was acquired at 380mm from the receiver.

Fig 8 shows the experimental received signals, superposed with numerically simulated signals, in the x-axis at both sides of the transmitter. As can be seen, the wave that propagates to the right is much stronger than the one that propagates to the left, experimentally confirming the unidirectional generation of the proposed design. The ratio of the peak-to-peak amplitude of the received waves at 0º and 180º was 12.0, higher than the reported in previous work, where the SH waves were generated by piezoelectric strips [9], and slightly lower than obtained with the side-shifted unidirectional SH-EMAT design [23]. The directivity diagram of the unidirectional transducer was also measured, both numerically and experimentally, and is shown in Fig. 9. In order to be consistent with the SH polarization and the signals acquired experimentally by the conventional PPM EMAT receiver, the numerical directivity was obtained from the tangential wavefield component, perpendicular to the radial direction at each angle. The tangential component was computed with the extracted x and z components of the wavefield on the surface of the plate at 380 mm from the center of the generation location, shown in Fig.4. Good agreement between simulation and experiments was obtained.

VI. Discussion

Some practical concerns have to be considered when fabricating the proposed unidirectional EMAT. First of all, attention should be paid to winding sense, which has to alternate between magnets of the same column, as shown in Fig. 3(a), so that forces are properly added since magnets have alternate polarity. Besides, in order to properly suppress the backward wave, the induced forces from each magnet and coil ideally have to be identical. The generated forces' distribution depends, principally, on the number of coil turns, the initial and ending position of the coil with respect to the magnets' width, and on the individual lift-off of each magnet. Providing extreme precision for all those parameters among all magnets and coils pairs is, however, challenging. While slight fabrication imprecisions in conventional EMATs are usually irrelevant, for the principle of operation in this paper to work, all force-inducing elements need to be as similar as possible, so that the destructive interference phenomenon properly occurs. Here, we successfully fabricate the unidirectional EMAT with three periods, and hence twelve columns of magnets, with a degree of precision that enabled us to confirm unidirectional behavior and providing a strong forward propagating wave.

It is worth noticing that, the present design does not appear to present any significant amplitude backward travelling side-lobes, as can be seen either in the left-hand semi-plane of Fig. 5 or from 90º to 270º in Fig. 9. The highest amplitude in this angular interval is found at 180º, which is 21.6 dB below the main forward lode. Backward side-lobes were a drawback of the unidirectional side-shifted PPM EMAT [23], which showed non-negligible back propagating waves, close to 150º and 210º, as high as about 8.2 dB below the main forward lobe, due to the wavefront diffraction produced by the side-shift (in the z-drection) between both arrays, necessary to accommodate the second array between the rows of the first, as illustrated in Fig. 2(b). In that design, since the wavefronts from each individual array were side-shifted, a complete destructive interference at the backward direction only occurred in the centerline (x-axis) of the transducer where the contribution of each wavefront are equal in amplitude and in opposite phase. At an angle from the x-axis the contribution of one wavefront stands-out over the other, not allowing a complete cancelation and thus creating the backwards side-lobes. In the present design, all sources are aligned in the z-direction, as shown in Fig.3(a), hence their contributions properly destructively interfere in the whole backward semi-plane, and thus the backward propagating side-lobes do not arise. Also, since the active width of the transducer is in the order of the wavelength, no forward side-lobe is neither observable [30].

VII. CONCLUSION

Unidirectional wave generation can simplify the analysis of received ultrasonic signals, avoiding unwanted reflected waves or multi-turn waves in closed-loop paths, making them of great interest for non-destructive evaluation applications. Typical PPM EMATs do not support a second independent source of forces in order to generate unidirectional SH waves by means of longitudinally-shifted and delayed line sources method. Here we have proposed a design of a unidirectional SH EMAT using the traditional PPM array, but with a dual linear-coil array instead of the common racetrack coil. The principle of operation relies on the interference of the generated waves from two alternate arrays, and thus the fabrication process has to be precise enough to ensure that all elements of the dual linear-coil array are wound as similar as possible, so that the forces produced by all of them are nominally identical, as well as ensuring that the proper winding sense is applied to each element.

Experiment and numerical simulation showed good agreement, and confirmed that the proposed solution is effective in generating SH waves that propagate in a single direction with around 20 dB unidirectionality, similar to or higher than obtained elsewhere. The wavefronts produced by each independent source are aligned, and thus provide ideally perfect interference, either constructive or destructive, generating unidirectional SH waves without backward propagating side-lobes, which can significantly reduce the probability of false alarm of an EMAT detection system.

REFERENCES

[1] M. Clough, M. Fleming and S. Dixon, "Circumferential guided wave EMAT system for pipeline screening using shear horizontal ultrasound," *NDT and E International,* vol. 86, p. 20 – 27, 2017.

[2] N. Suresh and K. Balasubramaniam, "Quantifying the lowest remnant thickness using a novel broadband wavelength and frequency EMAT utilizing the cut-off property of guided waves," *NDT & E International,* vol. 116, p. 102313, 2020.

[3] O. Trushkevych, M. Tabatabaeipour, S. Dixon, M. Potter, G. Dobie, C. MacLeod and R. Edward, "Miniaturised SH EMATs for fast robotic screening of wall thinning in steel plates," *IEEE Sensors Journal,* vol. 21, no. 0, pp. 1386-1394, 2021.

[4] A. C. Kubrusly, J. P. von der Weid and S. Dixon, "Experimental and numerical investigation of the interaction of the first four SH guided wave modes with symmetric and nonsymmetric discontinuities in plates," *NDT & E International,* vol. 108, p. 102175, 2019.

[5] A. C. Kubrusly, M. A. Freitas, J. P. von der Weid and S. Dixon, "Interaction of SH guided waves with wall thinning," *NDT & E International,* vol. 101, pp. 94-103, 2019.

[6] P. Khalili and F. Cegla, "Excitation of Single-Mode Shear-Horizontal Guided Waves and Evaluation of Their Sensitivity to Very Shallow Crack-Like Defects," *IEEE Transactions on Ultrasonics, Ferroelectrics, and Frequency Control,* p. Early Access, 2020.

[7] H. Miao and F. LI, "Shear horizontal wave transducers for structural health monitoring and nondestructive testing: A review," *Ultrasonics,* p. 106355, 2021.

[8] H. Miao, Q. Huan, F. Li and G. Kang, "A variable-frequency bidirectional shear horizontal (SH) wave transducer based on dual face-shear (d24) piezoelectric wafers,," *Ultrasonics,* vol. 89, pp. 13-21, 2018.

[9] M. Chen, Q. Huan and F. Li, "A unidirectional SH wave transducer based on phase-controlled antiparallel thickness-shear (d15) piezoelectric strips," *Theoretical and Applied Mechanics Letters,* vol. 10, no. 5, pp. 299-306, 2020,.

[10] G. Boivin, M. Viens and Belanger, "Plane Wave SH0 Piezoceramic Transduction Optimized Using Geometrical Parameters.," *Sensors,* vol. 18, no. 2, p. 542, 2018.

[11] Y. Kim and Y. E. Kwon, "Review of magnetostrictive patch transducers and applications in ultrasonic nondestructive testing of waveguide," *Ultrasonics,* vol. 62, pp. 3-19, 2015.

[12] K. Toda and Y. . Shinoda, "Unidirectional transducer with three electrode groups for Lamb- wave devices," *The Journal of the Acoustical Society of America,* vol. 63, no. 2, pp. 614-617, 1978.

[13] T. Yamasaki, S. Tamai and M. Hirao, "Arrayed-coil EMAT for longitudinal wave in steel wires," in *1998 IEEE*

Ultrasonics Symposium, Sendai, Japan, 1998.

[14] W. Zhu and J. L. Rose, "Lamb wave generation and reception with time-delay periodic linear arrays: a BEM simulation and experimental study," *IEEE Transactions on Ultrasonics, Ferroelectrics, and Frequency Control*, vol. 46, no. 3, pp. 654-664, 1999.

[15] W. Zhu, A. Chahbaz and M. Brassard, "Time-Delay Periodic Linear Array: A unidirectional guided wave transducer for ultrasonic NDT applications," *AIP Conference Proceedings* , vol. 509, no. 1, pp. 1057-1064 , 2000.

[16] W. Zhu, "A Finite Element Analysis of the Time-Delay Finite Element Analysis of the Time-DelPeriodic Ring Arrays for Guided Wave Generation and Reception in Hollow Cylinders," *IEEE Transactions on Ultrasonics, Ferroelectrics, and Frequency Control*, vol. 48, no. 5, pp. 1462--1470, 2001.

[17] D. N. Alleyne and P. Cawley, "Long range propagation of Lamb waves in chemical plant pipework," *Materials evaluation*, vol. 55, no. 4, pp. 504-508, 1997.

[18] X. Niu, K. F. T. Tee and l. M. H. R., "The Unidirectional Excitation of Guided Waves with an Increased Power Using Multiple Transducer Arrays in Pipelines for Structural Health Monitoring," in *Proceedings of the 12th International Workshop on Structural Health Monitoring (IWSHM 2019*, California, 2019.

[19] X. Niu, W. Duan, H.-P. Chen and l. M. H. R., "Excitation and propagation of torsional T(0,1) mode for guided wave testing of pipeline integrity," *Measurement*, vol. 131, pp. 341-348, 2019.

[20] X. Niu, K. Tee and H. R. Marques, "Enhancement of unidirectional excitation of guided torsional T(0,1) mode by linear superposition of multiple rings of transducers," *Applied Acoustics*, vol. 168, 2020.

[21] S. Wang, R. Su, X. Chen, L. Kang and G. Zhai, "Numerical and experimental analyis of unidirectional meander-line coil electromagnetic acoustic transducer," *IEEE Transactions on Ultrasonics, Ferroelectrics, and Frequency Control*, vol. 60, no. 12, pp. 2657 - 2664, 2013.

[22] X. Chen, R. Su, H. Zhang and G. Zhai, "Influence of coil parameters on transduction performance of unidirectional EMATs for Rayleigh wave," in *Far East Forum on Nondestructive Evaluation/Testing: New Technology and Application*, Jinan, 2013.

[23] A. C. Kubrusly, L. Kang and S. Dixon, "Unidirectional shear horizontal wave generation with side-shifted periodic permanent magnets electromagnetic acoustic transducer," *IEEE Transactions on Ultrasonics, Ferroelectrics, and Frequency Control*, vol. 67, no. 12, pp. 2757-276, 2020.

[24] J. L. Rose, Ultrasonic Guided waves in solid media, Cambridge University Press, 2014.

[25] M. Hirao and H. Ogi, EMATs for science and industry: noncontacting ultrasonic measurements, Springer, 2017.

[26] A. C. Kubrusly, M. A. Freitas, v. d. Weid and S. J. P. Dixon, "Mode Selectivity of SH Guided Waves by Dual Excitation and Reception Applied to Mode Conversion Analysis," *IEEE Transactions on Ultrasonics, Ferroelectrics, and Frequency Control*, vol. 65, no. 7, pp. 1239-1249, 2018.

[27] P. A. Petcher and S. Dixon, "Mode mixing in shear horizontal ultrasonic guided waves," *Nondestruct. Test. Eval.,*, vol. 32, no. 2, pp. 113-112, 2016.

[28] A. C. Kubrusly, P. Tovar, J. P. von der Weid and S. Dixon, "Mode conversion of SH guided waves with symmetry inversion in plates," *Ultrasonics*, vol. 112, p. 106334, 2021.

[29] A. Thon and P. Bélanger, "EMAT design for minimum remnant thickness gauging using high order shear horizontal modes," *Ultrasonics*, vol. 95, pp. 70-78, 2019.

[30] Q. Ma, J. Jiao, P. Hu, X. Zhong, B. Wu and C. He, "Excitation and detection of shear horizontal waves with electromagnetic acoustic transducers for nondestructive testing of plates," *Chinese Journal of Mechanical Engineering*, vol. 27, no. 2, p. 428–436, 2014.

[31] P. A. Petcher, S. E. Burrows and S. Dixon, "Shear horizontal (SH) ultrasound wave propagation around smooth corners," *Ultrasonics*, vol. 54, no. 4, pp. 997-1004, 2014.

[32] M. O. H. Hirao, "An SH-wave EMAT technique for gas pipeline inspection," *NDT&E International*, vol. 32, pp. 127-132, 1999.

[33] G.-F.-Q. Zhai, "Single SH Guided Wave Mode Generation Method for PPM EMATs," *Chinese Physics B*, vol. 29, no. 5, p. 054303, 2020.

[34] S. Choi, H. Cho and C. J. Lissenden, "Selection of Shear Horizontal Wave Transducers for Robotic Nondestructive Inspection in Harsh Environments," *Sensors*, vol. 17, no. 5, 2016.

[35] L. Xiang, D. D. S. Greenshields and R. S. Edwards, "Phased Electromagnetic Acoustic Transducer Array for Rayleigh Wave Surface Defect Detection," *IEEE Transactions on Ultrasonics, Ferroelectrics, and Frequency Control*, vol. 67, no. 7, pp. 1403-1411, 2020.

[36] C. Thring, S. J. Hill, S. Dixon and R. Edwards, "The effect of EMAT coil geometry on the Rayleigh wave frequency behaviour,," *Ultrasonics*, vol. 99, p. 105945, 2019.

[37] M. Rosli, R. Edwards and Y. Fan, "In-plane and out-of-plane measurements of Rayleigh waves using EMATs for characterising surface cracks," *NDT & E International*, vol. 49, pp. 1-9, 2012.

[38] O. V. Muraveva, V. V. Muravev and Y. V. Myshkin, "Laws of formation of grating lobes in the acoustic field of electromagnetic–acoustic transducers as a linear array of unidirectional conductors," *NDT & E International,*, vol. 93, pp. 40-56, 2018.